Fuzzy Logic based Admission Control for On-grid Energy Saving in Hybrid Energy Powered Cellular Networks

Heng Wang[1, 2], Chaowei Tang[2, *], Zhenzhen Zhao[3, 2] and Hui Tang[2]
[1] College of Mechanical and Electrical Engineering, Henan Agricultural University
Henan, 450002, China
[E-mail: wh1112009@163.com]
[2] College of Communication Engineering, Chongqing University
Chongqing, 400044, China
[E-mail: cwtang_cqu@163.com, tanghui@cqu.edu.cn]
[3] College of Computer and Information Engineering, Henan University of Economics and Law
Henan, 450002, China
[E-mail: zhenzhen715@163.com]
*Corresponding author: Chaowei Tang

Received October 21, 2015; revised June 30, 2016; accepted August 10, 2016; published October 31, 2016

Abstract

To efficiently reduce on-grid energy consumption, the admission control algorithm in the hybrid energy powered cellular network (HybE-Net) with base stations (BSs) powered by on-grid energy and solar energy is studied. In HybE-Net, the fluctuation of solar energy harvesting and energy consumption may result in the imbalance of solar energy utilization among BSs, i.e., some BSs may be surplus in solar energy, while others may maintain operation with on-grid energy supply. Obviously, it makes solar energy not completely useable, and on-grid energy cannot be reduced at capacity. Thus, how to control user admission to improve solar energy utilization and to reduce on-grid energy consumption is a great challenge. Motivated by this, we first model the energy flow behavior by using stochastic queue model, and dynamic energy characteristics are analyzed mathematically. Then, fuzzy logic based admission control algorithm is proposed, which comprehensively considers admission judgment parameters, e.g., transmission rate, bandwidth, energy state of BSs. Moreover, the index of solar energy utilization balancing is proposed to improve the balance of energy utilization among different BSs in the proposed algorithm. Finally, simulation results demonstrate that the proposed algorithm performs excellently in improving solar energy utilization and reducing on-grid energy consumption of the HybE-Net.

Keywords: Green communication, renewable energy, admission control, queuing theory, fuzzy logic

This work has been partly supported by National International Science and Technology Cooperation Project (2014DFA31560), Key Science Research Program of Henan Province (17A480004).

http://dx.doi.org/10.3837/tiis.2016.10.006 **ISSN : 1976-7277**

1. Introduction

With the explosive growth of wireless data traffic in cellular networks, several orders of magnitude base stations (BSs) have been deployed, and thus the relevant energy consumption and carbon emissions have increased explosively [1]. To reduce operational expenditures and carbon footprint, the main efforts of prior arts have been put in energy-efficient transmission, networking and radio resource allocation. For example, Niu et al. introduced the cell zooming mechanism to reduce energy consumption, which adjusted the cell radius according to traffic load distribution, user requirements and channel state information [2]. Bhaumik et al. proposed a multi-layer cellular architecture to adjust cell size for energy saving [3]. However, the possible economic and environmental gains brought by these pioneer works are bounded by the sole energy source, i.e., the fossil energy.

Recently, to use solar energy in powering cellular networks is widely accepted due to its pollution-free and renewable natures. In 3GPP technique specification [4], the use of renewable energy resources is explicitly encouraged by mobile networks. Moreover, companies, such as Ericsson and Alcatel-Lucent, have launched projects to exploit solar energy for cellular BSs [5]. However, as the availability and capacity of the solar energy are unreliable and unstable, solar energy may not guarantee sufficient energy supplies for the BS [6]. Thus, we envision future BSs in cellular networks to be powered by solar energy and on-grid energy, which will construct the hybrid energy powered cellular networks (HybE-Net). In HybE-Net, BSs are previously powered by solar energy, and when the harvested solar energy cannot provide sufficient power for the BS energy demand, on-grid energy is immediately switched to guarantee the cell coverage and users' quality of service (QoS).

In HybE-Net, solar energy, which is influenced by meteorological conditions, is unstable. Moreover, the traffic load also exhibits both temporal and spatial diversity. Thus, the fluctuation of solar energy harvesting and the indeterminacy of the BS energy consumption may result in the imbalance of solar energy utilization among BSs, i.e., some BSs may be surplus in solar energy, while others may maintain operation with on-grid energy supply. Obviously, it leads to the underutilized solar energy, and on-grid energy saving and carbon footprint reduction cannot be achieved at capacity. Therefore, how to narrow the solar energy utilization gap among BSs for on-grid energy saving is one of the greatest challenges.

As an important component in resource management for cellular networks, admission control has a notable effect on the utilization of network resources. Considering admission judgment parameters (e.g., traffic load, resource utilization, quality of communication service and etc.), the optimal BS is adopted for each mobile user to optimize the resource utilization of cellular networks. Therefore, on the basis of guaranteeing the quality of communication service, the solar energy utilization among different BSs can be balanced through controlling the admission of mobile users in HybE-Net to achieve the purpose of on-grid energy saving and carbon footprint reduction.

Nowadays, the main efforts of admission algorithms mainly focus on the impacts of network parameters, such as communication link quality, system available bandwidth, traffic load and time delay on the admission of mobile users. For example, Vergados et al. proposed an adaptive resource-allocation scheme for QoS provisioning in a wireless healthcare information system. Since the wireless network has multiple service types and multiple priorities, prioritization is essential and degradation and upgrade policies were considered to increase the overall performance [7]. Chowdhury et al. proposed an efficient call admission control algorithm that relies on adaptive multi-level bandwidth-allocation scheme for non-real-time calls [8]. Cruz-Perez et al. proposed new flexible resource-allocation strategies that cope with scenarios with multiple service types and multiple priorities. The concepts of prioritized call degradation and compensation, and a call-admission mechanism that rejects calls originated by low-priority service types were introduced to achieve the proposed strategies [9]. Khanjari et al. presented an adaptive call admission control scheme that uses complete sharing approach of the available bandwidth among all traffic classes for multi-class service wireless cellular networks [10]. However, existing works ignore analysis on the solar energy state of BSs. Moreover, they did not well research out the best tradeoff among different factors, such as terminal business demand, network parameters and solar energy states of BSs, from the perspective of energy conservation and emission reduction. Hence, considering that BSs in different locations have different energy harvesting abilities, the traditional algorithms obviously could not deal with the admission control and resource optimization problems for HybE-Net. Therefore, a new admission control algorithms must be designed, and some problems should be comprehensively considered:

1) In HybE-Net, BSs in different locations have different energy harvesting abilities and traffic load, and then how to analyze and quantify the solar energy state and dynamic characteristics of different BSs;

2) How to assess the influences of accessing mobile users to different BSs on the balance of solar energy utilization in HybE-Net;

3) On the basis of comprehensively considering admission factors, e.g., communication link quality, system available bandwidth, traffic load and solar energy states of BSs, how to propose an admission control algorithm to effectively balance the solar energy utilization in HybE-Net.

In this paper, we proposed the admission control algorithm for HybE-Net. Firstly, solar energy states and dynamic characteristics of BSs are analyzed using the diffusion approximation theory. Then, we comprehensively consider admission judgment parameters, such as data transmission rate, available bandwidth and solar energy states of BSs, using the fuzzy logic theory. In the meantime, the index of solar energy utilization balancing is proposed to balance the solar energy utilization among different BSs in the proposed admission control algorithm. Specifically, the main contributions are described as follows:

1) In HybE-Net, unstable availability of solar energy flow of the BS is a great challenge. Considering the fluctuation of energy harvesting and the indeterminacy of energy consumption, energy flow behavior of the BS is firstly modeled as M/G/1/K. Then, the energy dynamic characteristics are analyzed by adopting the diffusion approximation method.

2) The index of solar energy utilization balancing is proposed to evaluate the influences of user admission to different BSs on the balance of solar energy utilization.

3) Based on guaranteeing the quality of communication service, a fuzzy logic based admission control algorithm is proposed, which performs excellently in improving the balance of solar energy utilization among BSs, saving on-grid energy and reducing carbon emissions in HybE-Net.

The rest of this paper is structured as follows. Mathematical models of the HybE-Net are provided in Section 2. In Section 3, energy flow behavior of the system is modeled as a stochastic queue. Based on the constructed model, energy behavior characteristics are analyzed mathematically. In Section 4, a fuzzy logic based admission control algorithm is proposed. Results and analyses are presented in Section 5. Finally, Section 6 provides the conclusion.

2. System Model

2.1 Network Scenario

As illustrated in **Fig. 1**, BSs in the HybE-Net are powered by solar energy and on-grid energy, which are called the hybrid energy powered BS (HybE-BS). The typical HybE-BS system comprises photovoltaic (PV) panels, a battery bank, an energy management system and the BS. In the HybE-BS, energy flow generated by PV panels flows into the battery bank and then is extracted to feed the BS energy demand. When the harvested solar energy cannot provide sufficient power for the BS, on-grid energy is immediately switched by the energy management system to guarantee the cell coverage and users' QoS. Moreover, each HybE-BS has the dedicated PV panels and battery bank, and the harvested energy cannot be shared among them.

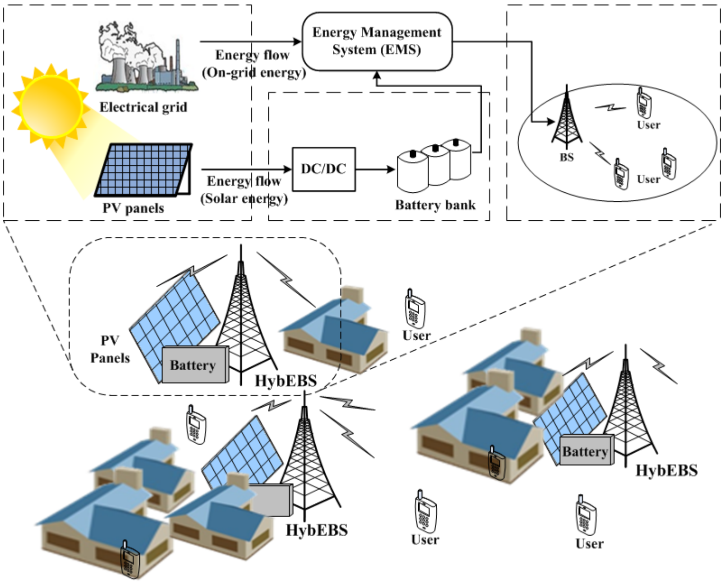

Fig. 1. Schematic diagram of hybrid energy powered cellular networks

2.2 Solar Energy Harvesting Model

As the green energy generator, PV panels convert solar energy into electrical power via photovoltaic effect. Depending on changeable meteorological conditions (i.e., solar irradiance and ambient temperature), the output energy of PV panels is highly dynamic and unstable. According to [11], the photovoltaic output power P_{pan} can be given by

$$P_{\text{pan}} = P_{\text{pan}}^{*} \cdot \eta_{\text{pan}} \cdot \frac{G}{G^{*}} \cdot \left[1 + a_{\text{T}} \cdot (T_{\text{amb}} + 0.02 \cdot G - T_{\text{pan}}^{*})\right], \tag{1}$$

where P_{pan}^{*} is the rated output power of PV panels under standardized test conditions (STC); η_{pan} is the energy conversion efficiency of PV panels; G^{*} is the solar irradiance under STC and equals 1,000 W/m^2; G is the solar irradiance; a_{T} indicates the temperature coefficient; T_{amb} is the ambient temperature; T^*_{pan} is the panel temperature under STC and equals 25°C. Obviously, the photovoltaic output power is mainly determined by the solar irradiance and the ambient temperature. Moreover, during the period $[0,T]$, the solar energy harvesting rate λ_e is calculated by $\lambda_e = \int_0^T P_{\text{pan}}(\tau)d\tau$.

2.3 Energy Consumption Model

The power consumption of HybE-BS i, which can be abstracted into the static power consumption P_i^{sta} and the dynamic power consumption P_i^{dyn}, is expressed as

$$P_i = P_i^{\text{dyn}} + P_i^{\text{sta}}. \tag{2}$$

During the period $[0,T]$, the number of active users served by HybE-BS i is denoted as $\mathcal{M}$. Thus, the dynamic power consumption of HybE-BS i can be calculated by

$$P_i^{\text{dyn}} = \sum_{m=1}^{\mathcal{M}} \frac{P_{i,m}^{\text{tr}}}{\eta_{\text{PA}}}, \tag{3}$$

where $P_{i,m}^{\text{tr}}$ is the transmission power of power amplifier over link between user m and HybE-BS i; η_{PA} is the power amplifier efficiency. Based on path loss model and Shannon theory, $P_{i,m}^{\text{tr}}$ can be further expressed by

$$P_{i,m}^{\text{tr}} = \sigma_0 \cdot \kappa \cdot d_{i,m}^{\psi} (2^{\frac{r_{\min}}{w}} - 1), \tag{4}$$

where σ_0 is power spectral density of white Gaussian noise; w is bandwidth; κ is a parameter of the path loss model; ψ is the path loss exponent; $r_{\min}$ is the minimum transmission rate and $d_{i,m}$ is the distance between user m and the HybE-BS i.

Based on the above analysis, during the period $[0,T]$ the power consumption of HybE-BS i can be rewritten by

$$P_i = P_i^{\text{sta}} + \sum_{m=1}^{\mathcal{M}} \frac{\sigma_0 \cdot \kappa \cdot d_{i,m}^{\psi} (2^{\frac{r_{\min}}{w}} - 1)}{\eta_{\text{PA}}}. \tag{5}$$

Correspondingly, the energy consumption of the HybE-BS i is expressed as

$$E_i^c = P_i^{\text{sta}} \cdot T + \sum_{m=1}^{\mathcal{M}} t_m \cdot \frac{\sigma_0 \cdot \kappa \cdot d_{i,m}^{\psi} (2^{\frac{r_{\min}}{w}} - 1)}{\eta_{\text{PA}}}, \tag{6}$$

where t_m is a random variable and represents the service time of user m. Thus, the mean and variance of E_i^c, denoted as $\tilde{u}_i^c$ and $\tilde{v}_i^c$, are given by

$$\begin{cases} \tilde{u}_i^c = \mathbb{E}\left[E_i^c\right] = P_i^{\mathrm{sta}} \cdot T + \sum_{m=1}^{\mathcal{M}} \mathbb{E}[t_m] \cdot \dfrac{\sigma_0 \cdot \kappa \cdot d_{i,m}^{\psi} (2^{\frac{r_{\min}}{w}} - 1)}{\eta_{\mathrm{PA}}}, \\ \tilde{v}_i^c = \mathbb{D}\left[E_i^c\right] = \sum_{m=1}^{\mathcal{M}} \mathbb{D}[t_m] \cdot \left[\dfrac{\sigma_0 \cdot \kappa \cdot d_{i,m}^{\psi} (2^{\frac{r_{\min}}{w}} - 1)}{\eta_{\mathrm{PA}}}\right]^2. \end{cases} \tag{7}$$

where $\mathbb{E}[t_m]$ and $\mathbb{D}[t_m]$ are the mean and variance of the service time of user m, respectively. Correspondingly, the mean and variance of energy consumption rate of HybE-BS i are denoted as u_i^c and v_i^c. They are calculated by $u_i^c = \tilde{u}_i^c / T$ and $v_i^c = \tilde{v}_i^c / T^2$.

3. Modeling and Analysis of Solar Energy Flow Behavior

In HybE-Net, admission control should consider not only the network parameters, e.g., communication link quality, bandwidth, transmission rate, but also energy dynamic characteristics of the HybE-BS. Thus, the solar energy state and dynamic characteristics of the HybE-BS are analyzed mathematically.

3.1 Stochastic Queue Modeling for Energy Flow Behavior in Solar Energy Supply

According to the type of energy source, there are two energy supply forms in HybE-BS, i.e., on-grid energy supply and solar energy supply. In solar energy supply, recalling the solar energy flow depicted in **Fig. 1**, the battery bank is utilized to bridge the energy harvesting (arrival) and energy consumption (departure) process, c.f. **Fig. 2**. Ng et al. showed that solar energy arrivals can be viewed as a Poisson process [12]. Then, the energy harvesting process can be proven to be a Poisson process due to the deterministic power output model of PV panels. Meanwhile, the energy consumption process which depends on plenty of random factors (e.g., traffic load characteristics) is also regarded as a random process. Moreover, owing to the finite capacity of the lithium battery bank, the newly harvested energy units cannot be stored and have to be discarded immediately when the battery bank is full. Therefore, the energy flow behavior of the solar energy supply can be modeled as an M/G/1/K queue. Note that the capacity of the battery bank is represented to be K energy units.

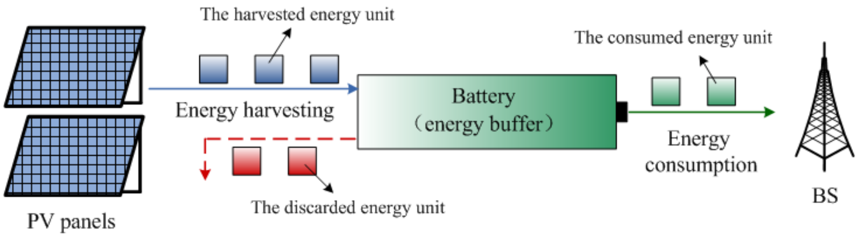

Fig. 2. Energy queue model in solar energy supply.

3.2 Solar Energy State Analysis

Because the battery bank is the unique energy storage device in HybE-BS, its energy state can be directly reflected by the amount of energy stored in the battery bank. Based on the constructed model, the energy state of HybE-BS i at the time k can be given by

$$e_i(k)=\min\left\{\max\left\{e_i(k-1)+E_i^{\mathrm{H}}(k)-E_i^{\mathrm{C}}(k),0\right\},e_i^{\max}\right\}, \tag{8}$$

where $E_i^{\mathrm{H}}(k)$ and $E_i^{\mathrm{C}}(k)$ are the amount of the harvested energy and the consumed energy at time k. $e_i^{\max}$ is the maximum storage capacity of the battery bank.

Because the mathematical methods associated with the continuum make analytical treatment easier than those associated with discrete coordinate axes, the discrete energy state $e_i(k)$ is replaced by a continuous one $X_i(t)$. By the diffusion approximation approach, $X_i(t)$ can be modeled as the Brownian motion [13]

$$dX_i(t)=X_i(t+dt)-X_i(t)=\beta_i dt+\Psi(t)\sqrt{\alpha_i dt}, \tag{9}$$

where $\Psi(t)$ is a normally distributed random variable with zero mean and unit variance. α_i and β_i are diffusion coefficients of $X_i(t)$. They are calculated by

$$\begin{cases}\alpha_i=(u_i^h)^3\big/v_i^h+(u_i^c)^3\big/v_i^c\\ \beta_i=u_i^h-u_i^c\end{cases}, \tag{10}$$

where u_i^c and v_i^c are the mean and variance of energy consumption rate of HybE-BS i. u_i^h and v_i^h are the mean and variance of energy harvesting rate of HybE-BS i. As the energy harvesting process can be modeled as a Poisson process, $u_i^h=v_i^h$.

When a continuous energy flow process $X_i(t)$ starts at the initial energy state x_0, the conditional probability density function (PDF) of the energy state x at time t can be represented by

$$g_i(x,t;x_0,e_i^{\max})=\Pr(x\le X_i(t)<x+dx\,|\,x_0,e_i^{\max}). \tag{11}$$

With the diffusion approximation, $g_i(x,t;x_0,e_i^{\max})$ can be characterized by the forward diffusion equation [14],

$$\begin{aligned}\frac{\partial g_i(x,t;x_0,e_i^{\max})}{\partial t}&=\frac{\alpha_i}{2}\frac{\partial^2 g_i(x,t;x_0,e_i^{\max})}{\partial e^2}-\beta_i\frac{\partial g_i(x,t;x_0,e_i^{\max})}{\partial e}\\&\quad+\frac{P_{i,0}(t;x_0,e_i^{\max})\delta(x-1)}{u_i^h}+\frac{P_{i,e_i^{\max}}(t;x_0,e_i^{\max})\delta(x-e_i^{\max}+1)}{u_i^c}.\end{aligned} \tag{12}$$

In Eq. (12),

$$\begin{cases}P_{i,0}(t;x_0,e_i^{\max})=\Pr\left[X_i(t)=0\,|\,X_i(0)=x_0,e_i^{\max}\right]\\ P_{i,e_i^{\max}}(t;x_0,e_i^{\max})=\Pr\left[X_i(t)=e_i^{\max}\,|\,X_i(0)=x_0,e_i^{\max}\right]\end{cases}, \tag{13}$$

which are respectively the probability mass functions at the boundaries $x=0$ and $x=e_i^{\max}$. Meanwhile, they should also satisfy the following equations:

$$\frac{dP_{i,0}(t;x_0,e_i^{\max})}{dt}=-\frac{P_{i,0}(t;x_0,e_i^{\max})}{u_i^h}+\lim_{x\to 0}\left[\frac{\alpha_i}{2}\frac{\partial g_i(x,t;x_0,e_i^{\max})}{\partial e}-\beta_i g_i(x,t;x_0,e_i^{\max})\right], \tag{14}$$

$$\frac{dP_{i,e_i^{\max}}(t;x_0,e_i^{\max})}{dt}=-\frac{P_{i,e_i^{\max}}(t;x_0,e_i^{\max})}{\mu_i^h}+\lim_{x\to e_i^{\max}}\left[-\frac{\alpha_i}{2}\frac{\partial g_i(x,t;x_0,e_i^{\max})}{\partial x}+\beta_i g_i(x,t;x_0,e_i^{\max})\right]. \tag{15}$$

They are subject to the initial condition $g_i(x,t;x_0,e_i^{\max})=\delta(x-x_0)$ and boundary conditions $\lim_{x\to 0} g_i(x,t;x_0,e_i^{\max})=0$ and $\lim_{x\to e_i^{\max}} g_i(x,t;x_0,e_i^{\max})=0$.

By applying the method of images [13], the transient solution of Eq. (12) is obtained by

$$g_i(x,t;x_0,e_i^{\max})=\frac{1}{\sqrt{2\pi\alpha_i t}}\sum_{n=-\infty}^{\infty}\left(A_n-B_n\right),\quad t>0, \tag{16}$$

where

$$\begin{cases} A_n=\exp\left[\dfrac{2n\cdot e_i^{\max}\cdot\beta_i}{\alpha_i}-\dfrac{\left(x-x_0-2n\cdot e_i^{\max}-\beta_i\cdot t\right)^2}{2\alpha_i t}\right], \\ B_n=\exp\left[\dfrac{\left(-2n\cdot e_i^{\max}-2x_0\right)\cdot\beta_i}{\alpha_i}-\dfrac{\left(x+x_0+2n\cdot e_i^{\max}-\beta_i\cdot t\right)^2}{2\alpha_i t}\right]. \end{cases} \tag{17}$$

Correspondingly, the mean of solar energy state of HybE-BS i is expressed as

$$\mathbb{E}\left[g_i(x,t;x_0,e_i^{\max})\right]=\sqrt{\frac{\alpha_i t}{2\pi}}\sum_{n=-\infty}^{\infty}\left(\bar{A}_n-\bar{B}_n\right)\qquad t>0, \tag{18}$$

where

$$\begin{cases} \bar{A}_n=\sqrt{\pi}\left(x_0+2n\cdot e_i^{\max}+\beta_i\cdot t\right)-A_n\Big|_0^{e_i^{\max}}; \\ \bar{B}_n=\sqrt{\pi}\left(x_0-2n\cdot e_i^{\max}+\beta_i\cdot t\right)-B_n\Big|_0^{e_i^{\max}}. \end{cases} \tag{19}$$

3.3 Solar Energy Supply Duration Analysis

Solar energy supply duration is the period during which solar energy is consumed from the initial energy state $X(0)=x_0$ to $X(t)=0$. The PDF of solar energy supply duration $\mathcal{T}_i(x,x_0)$ is obtained from the diffusion equation with the absorbing barrier at the origin,

$$g_{\mathcal{T}_i}(t;x_0,e_i^{\max})=\lim_{x\to 0}\left[\frac{\alpha_i}{2}\frac{\partial g_i(x,t;x_0,e_i^{\max})}{\partial x}-\beta_i g_i(x,t;x_0,e_i^{\max})\right]. \tag{20}$$

Then, the mean of the solar energy supply duration of HybE-BS i is expressed as

$$\mathbb{E}\left[\mathcal{T}_i(0,x_0)\right]=\begin{cases}-\dfrac{x_0}{\beta_i}+\left(\dfrac{1}{\mu_i^h}+\dfrac{1}{\beta_i}\right)\dfrac{\exp\left\{-\dfrac{2\left(e_i^{\max}-x_0\right)\beta_i}{\alpha_i}\right\}-\exp\left\{-\dfrac{2e_i^{\max}\beta_i}{\alpha_i}\right\}}{1-\exp\left\{-\dfrac{2\beta_i}{\alpha_i}\right\}}, & \beta_i\neq 0;\\ x_0\cdot\left(\dfrac{1}{\mu_i^h}+\dfrac{2e_i^{\max}-x_0-1}{\alpha_i}\right), & \beta_i=0.\end{cases}$$

(21)

3.4 Solar Energy Depleting Probability Analysis

Solar energy depleting probability indicates that solar energy is depleted at $t\to\infty$. To facilitate the analysis, $\lim_{t\to\infty} g_i(x,t;x_0,e_i^{\max})$ is represented by $g_i(x;x_0,e_i^{\max})$, and $\lim_{t\to\infty} P_{i,0}(t;x_0,e_i^{\max})$ and $\lim_{t\to\infty} P_{i,e_i^{\max}}(t;x_0,e_i^{\max})$ are represented by $P_{i,0}$ and $P_{i,e_i^{\max}}$. Thus, the PDF of the solar energy state is given by

$$\frac{\alpha_i}{2}\frac{\partial^2 g_i(x;x_0,e_i^{\max})}{\partial x^2}-\beta_i\frac{\partial g_i(x;x_0,e_i^{\max})}{\partial x}=-\frac{P_{i,0}\delta(x-1)}{\mu_i^h}-\frac{P_{i,e_i^{\max}}\delta(x-e_i^{\max}+1)}{\mu_i^c}. \quad (22)$$

The transient solution of Eq. (22) can be obtained by

$$g_i(x;x_0,e_i^{\max})=\begin{cases}-\dfrac{P_{i,0}}{\mu_i^h\cdot\beta_i}\left[1-e^{\gamma_i\cdot x}\right], & 0\le x\le 1\\ -\dfrac{P_{i,0}}{\mu_i^h\cdot\beta_i}\left[e^{-\gamma_i}-1\right]e^{\gamma_i\cdot x}, & 1\le x\le e_i^{\max}-1\\ -\dfrac{P_{i,0}}{\mu_i^h\cdot\beta_i}\left[e^{\gamma_i\left(x-e_i^{\max}\right)}-1\right]e^{\gamma_i\cdot\left(e_i^{\max}-1\right)}, & e_i^{\max}-1\le x\le e_i^{\max}\end{cases} \quad (23)$$

where $\gamma_i=2\cdot\beta_i/\alpha_i$. Then, solar energy depleting probability is given by

$$\mathcal{P}_i=\begin{cases}\left\{1+\dfrac{\mu_i^h}{\mu_i^c-\mu_i^h}+\dfrac{\mu_i^h}{\mu_i^c}\exp\left[\gamma_i\left(e_i^{\max}-1\right)\right]-\dfrac{\mu_i^h}{\mu_i^c-\mu_i^h}\exp\left[\gamma_i\left(e_i^{\max}-1\right)\right]\right\}^{-1}, & \beta_i\neq 0;\\ \dfrac{1}{2}\left[1+\dfrac{e_i^{\max}-1}{\left(\mu_i^h/v_i^h\right)^2+\left(\mu_i^c/v_i^c\right)^2}\right]^{-1}, & \beta_i=0.\end{cases}$$

(24)

4. Fuzzy Logic based Admission Control Algorithm

In HybE-Net, admission control algorithm comprehensively analyzes admission judgment parameters, e.g., communication link quality, available bandwidth and solar energy states of BSs, and then provides an optimal network for mobile users. Obviously, it is a multi-factor decision-making process which contains characteristics of various levels and demands from users and network. Traditional multi-factor decision-making processes [15-16] are mainly depending on the exact value of judgment parameters, while these parameters in real life are always featured with fuzziness. For instance, "the communication link quality is relatively good", "the solar energy is not sufficient". These expressions are in strong subjectivity, which cannot be expressed with exact values. However, as a discipline developed to solve the fuzzy phenomenon in real life, fuzzy logic [17] is a mathematical method to exactly solve the inexact and incomplete information problem. Therefore, targeting at the fuzzy and uncertain problem of admission control process in HybE-Net, this paper puts forward an effective admission control method based on fuzzy logic.

The fuzzy logic control includes three stages: fuzzification, fuzzy inference and defuzzification. According to the user's service demand and HybE-Net characteristics, we select transmission rate, available bandwidth and solar energy states of BSs as the admission judgment parameters, and then fuzzy logic is employed to analyze these mentioned parameters. Subsequently, the index of solar energy utilization balancing is proposed to assess the changes of solar energy utilization balance when mobile users access to different HybE-BSs. The proposed algorithm is illustrated as follows.

1) Judgment parameters fuzzification

Transmission rate intuitively reflects the communication link quality between users and HybE-BSs, and it is determined by the transmitting power of BS and the path loss. Thus, transmission rate is adopted to be one of judgment parameters in the admission control algorithm.

Assume user m lies in the overlapping coverage region of I HybE-BSs. Then, according to Eq. (4), the transmission rate $r_{i,m}$ over the link between user m and its anchored HybE-BS i ($i = 1, 2, \cdots I$) can be obtained by:

$$r_{i,m} = w \cdot \log_2\left(1 + \frac{P_i^{\mathrm{tr}}}{\sigma_0 \cdot \kappa \cdot d_{i,m}^{\psi}}\right). \quad (25)$$

where P_i^{tr} represents the transmission power of HybE-BS i; σ_0 is power spectral density of white Gaussian noise; w is bandwidth; κ is a parameter of the path loss model; ψ is the path loss exponent, $d_{i,m}$ is the distance between user m and the HybE-BS i.

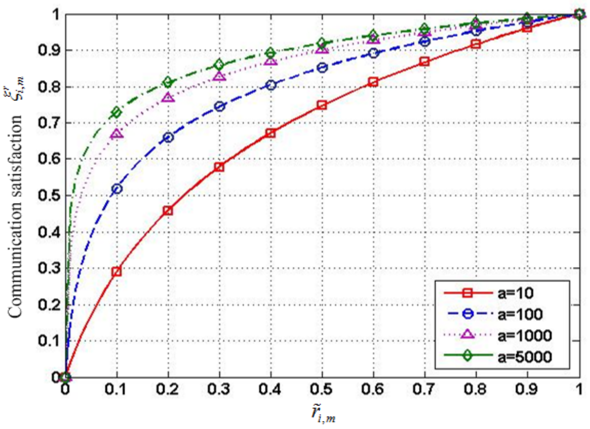

Fig. 3. Communication satisfaction under different normalized transmission rates.

Communication satisfaction, denoted as $\xi_{i,m}^{r}$, is used to reflect the actual situation of communication link quality, which is closely related to the received transmission rate. Obviously, the larger the communication satisfaction is, the faster the data transmission rate is. Specifically, communication satisfaction is defined as

$$\xi_{i,m}^{r} = \frac{\ln(1 + a \cdot \tilde{r}_{i,m})}{\ln(1+a)}, \tag{26}$$

where $\tilde{r}_{i,m}$ is the normalized transmission rate, and $\tilde{r}_{i,m} = r_{i,m} \Big/ \sum_{i=1}^{I} r_{i,m}$; a is satisfaction regulatory factor. Communication satisfaction corresponding to different normalized transmission rates is elaborated in **Fig. 3**. When $\tilde{r}_{i,m}$ value is small, the change of curve slope is relatively large, and vice versa. This phenomenon indicates that when the normalized transmission rate is relatively small, it is easy to distinguish the communication satisfaction among different HybE-BSs. However, when the normalized transmission rate is large, which means when the transmission rate can satisfy the communication quality well, the improvement of transmission rate will not lead to the significant rise in communication satisfaction. Therefore, the larger the communication satisfaction value of $\xi_{i,m}^{r}$ is, the better the communication link quality between user m and HybE-BS i is.

Network traffic load is another important parameter affecting admission control, which is directly reflected by the available bandwidth of BS. Assume the total bandwidth of HybE-BS i is W_i, and then the available bandwidth $\tilde{W}_i$ can be expressed as:

$$\tilde{W}_i = W_i - w \cdot N_i, \tag{27}$$

where N_i is the number of user served by the HybE-BS i. To facilitate analysis, the available bandwidth $\tilde{W}_i$ of the HybE-BS can be replaced by the available bandwidth ratio ξ_i^{w} ($0 \le \xi_i^{w} \le 1$) which refers to the proportion of available bandwidth to the total bandwidth. It is expressed as

$$\xi_i^{w} = \frac{\tilde{W}_i}{W_i} = \frac{W_i - w \cdot N_i}{W_i}. \tag{28}$$

Obviously, the larger the available bandwidth ratio is, the lighter the traffic load of the HybE-BS is.

In addition, solar energy station of the HybE-BS is also a vital factor influencing the admission judgment. In HybE-Net, to improve the solar energy utilization and reduce on-grid energy consumption, the admission judgment encourages users to access to the HybE-BS with sufficient solar energy. To facilitate analysis, the mean value of solar energy state in HybE-BS i is normalized by

$$\xi_i^{s} = \mathbb{E}\left[g_i(x, t; x_0, e_i^{\max}) \right] \Big/ e_i^{\max}. \tag{29}$$

Based on users' service demand and HybE-Net characteristics, communication satisfaction ξ_m^{r}, available bandwidth ratio ξ^{w} and the normalized solar energy state of the HybE-BS ξ^{s} are adopted as the input linguistic variables. To achieve a good balance between the accuracy of analysis and the amount of calculation, the input linguistic variable is divided into three fuzzy sets. They are expressed as below:

$$\begin{cases} \mathrm{T}\left(\xi_m^r\right)=\mathrm{T}\{\text{Weak,Medium,Strong}\}; \\ \mathrm{T}\left(\xi^w\right)=\mathrm{T}\{\text{Low,Medium,High}\}; \\ \mathrm{T}\left(\xi^s\right)=\mathrm{T}\{\text{Weak,Medium,Strong}\}. \end{cases} \tag{30}$$

Furthermore, evaluating admission judgment parameters by fuzzy logic model, the judgment result is divided into 5 linguistic terms: access (A), weak access (WA), not access not reject (NANR), weak reject (WR) and reject (R). Thus, the fuzzy set of output variable $h^{\mathrm{A/R}}$ can be expressed as $\mathrm{T}\left(h^{\mathrm{A/R}}\right)=\mathrm{T}\{\mathrm{R,WR,NANR,WA,A}\}$.

The fuzzification process is the process of solving different judgment parameters to belong to the membership of different fuzzy sets through the membership function. The membership function is the building blocks of fuzzy set theory, i.e., fuzziness in a fuzzy set is determined by its membership function. Accordingly, the shape of membership function is important for a particular problem since they have a profound effect on a fuzzy inference system [18]. In our studies, the sensitivity, robustness and response of fuzzy-controlled system with the triangular, trapezoidal and Gaussian membership function are compared. Gaussian membership function showed promising result in comparison to other membership functions, and it has been successfully utilized in past works [19, 20]. Therefore, the Gaussian function is selected as the membership function of various fuzzy set.

$$f_{j,k}\left(\mathcal{H}_j\right)=\exp\left[-\frac{(\mathcal{H}_j-b_{j,k})^2}{\tilde{\sigma}_{j,k}^2}\right], \tag{31}$$

where $\mathcal{H}_j$ ($j=1,2,3,4$) are respectively the input variables ξ_m^r, ξ^w, ξ^s, and the output variable $h^{\mathrm{A/R}}$; k is the kth fuzzy set of the $\mathcal{H}_j$; $b_{j,k}$ and $\tilde{\sigma}_{j,k}^2$ are the corresponding mean value and variance of the Gaussian membership function respectively. Gaussian membership functions in the proposed algorithm are shown in **Fig. 4**.

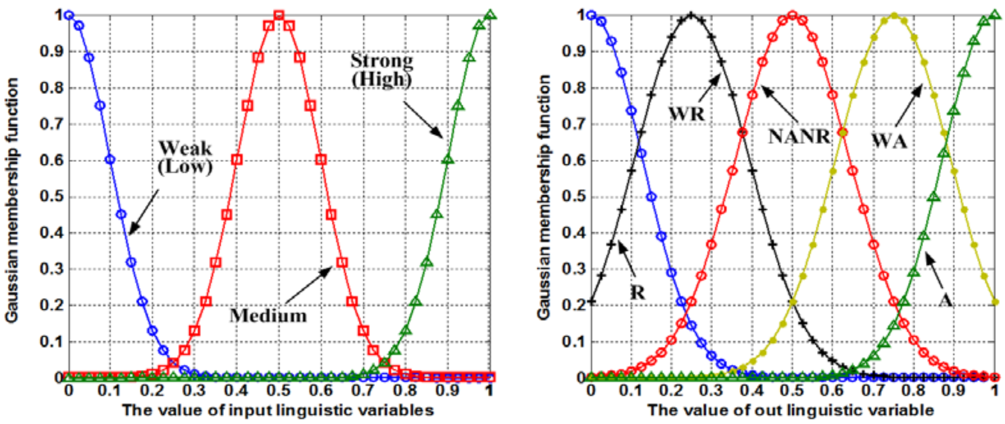

Fig. 4. Gaussian membership functions

2) Fuzzy inference rules establishment

Fuzzy inference rule is used to determine the relationship between linguistic variables and output variables. According to the actual experience, fuzzy inference rule is established from the aspect of guaranteeing communication quality and reducing on-grid energy consumption, as shown in **Table 1**. In our study, the inference is based on the Mamdani's method [21].

Table 1. Fuzzy inference rules

Communication satisfaction ξ_m^r	Available bandwidth ξ^w	Solar energy state ξ^s		
		Weak	Medium	Strong
Weak	Low	R	WR	NANR
	Medium	WR	NANR	WA
	High	WR	NANR	WA
Medium	Low	WR	NANR	WA
	Medium	WR	WA	A
	High	WA	A	A
Strong	Low	WR	WA	WA
	Medium	NANR	A	A
	High	WA	A	A

3) Defuzzification

In the fuzzy logic, defuzzification is a process transforming the fuzzy output value obtained from fuzzy inference into the exact judgment value. In the proposed algorithm, the center of gravity (CoG) [21] is employed to defuzzify the judgment result. In this paper, $h_{i,m}$ is denote as the judgment (output) value of user m accessing to BS i, which is obtained by fuzzy logic.

4) Admission judgment based on the index of solar energy utilization balancing

The admission control algorithm in HybE-Net need to consider not only communication link quality, available bandwidth and solar energy state of HybE-BSs, but also the balance of solar energy utilization among HybE-BSs. Therefore, the index of solar energy utilization balancing is defined to measure the balance degree of solar energy state among HybE-BSs, which can be specifically expressed as:

$$\theta_i^e = \left(\sum_{i=1}^{I} \mathcal{P}_i\right)^2 \Bigg/ \left(I \cdot \sum_{i=1}^{I} \mathcal{P}_i^2\right), \tag{32}$$

In Eq. (32), $\mathcal{P}_i$ is the solar energy depleting probability of HybE-BS i, which is calculated by Eq. (24). By analyzing the above formula, it is observed that when θ^e approaches to 1, solar energy depleting probability of every HybE-BS tends to be balanced. However, when θ^e approaches to $1/I$, solar energy depleting probability of every HybE-BSs is unbalanced. Obviously, the larger the θ^e is, the more beneficial to the balance of network solar energy utilization for user m accessing to HybE-BS i will be.

Therefore, as another judgment value, $l_{i,m}$ is defined as the normalized value of the index of solar energy utilization balancing,

$$l_{i,m} = \theta_i^{\mathrm{e}} \bigg/ \sum_{i=1}^{I} \theta_i^{\mathrm{e}} . \tag{33}$$

5) Admission control algorithm in HybE-Net

According to above analysis, admission judgment values of user m accessing to BS i, $h_{i,m}$ and $l_{i,m}$, are obtained by using the fuzzy logic method and calculating the index of solar energy utilization balancing. When $h_{i,m}$ is the larger value, it indicates that user m accessing to HybE-BS i has the better communication link quality, bandwidth resource and solar energy supply. However, when $l_{i,m}$ is the larger value, it indicates that user m accessing to HybE-BS i is more beneficial to balance solar energy utilization among different HybE-BSs. Therefore, the integrated admission judgment value, denoted as $L_{i,m}$, is defined as the smaller one between $h_{i,m}$ and $l_{i,m}$,

$$L_{i,m} = \min\left(h_{i,m}, l_{i,m}\right). \tag{34}$$

Assume user m lies in the overlapping coverage region of I HybE-BSs. With the above approach, the integrated admission judgment values $L_{i,m}\left(i = 1, 2, \cdots, I\right)$ can be obtained. Obviously, the HybE-BS with the largest integrated admission judgment value is the best access HybE-BS for user m. The pseudo code of the proposed admission control is shown in algorithm 1.

Computational complexity is usually used to describe an algorithm's use of computational resources. In the fuzzy inference process, fuzzy judgment results are calculated according to the fuzzy inference rule. The number of fuzzy inference rule is N^{r}, and thus the computing time complexity in this period is $O\left(N^{\mathrm{r}}\right)$. Meanwhile, the algorithm analyzes the integrated admission judgment result of I HybE-BSs. Therefore, the computational complexity of the proposed algorithm is $O\left(I \times N^{\mathrm{r}}\right)$.

Algorithm 1 Fuzzy logic based admission control algorithm

1: Calculate the mean and variance of energy harvesting rate, and set the transmission power P_i^{tr} and the total bandwidth W_i;
2: Provide the linguistic variables and output variables of the fuzzy set;
3: Provide the fuzzy inference rules;
4: For $i = 1$ to I do
5: Calculate $\xi_{i,m}^{r}$ according to Eq.(26);
6: Calculate ξ_i^{w} according to Eq.(28);
7: Calculate ξ_i^{s} according to Eq.(29);
8: Calculate the membership of input and output linguistic variables according to Eq.(31);
9: Obtain the judgment result according to the fuzzy inference rules;
10: Obtain $h_{i,m}$ by using the center of gravity method;

11: Calculate $l_{i,m}$ according to Eq.(33);

12: Compare $h_{i,m}$ and $l_{i,m}$, and then $L_{i,m} = \min\left(h_{i,m}, l_{i,m}\right)$

13: End for

14: Obtain the best admission HybE-BS $\tilde{i}$, $L_{\tilde{i},m} = \max\{L_{i,m}\}\left(i = 1, 2, \cdots, I\right)$;

15: Update $\xi_{\tilde{i}}^{w}$ and ξ_{i}^{s};

16: Return: $\tilde{i}$;

5. Simulation Result and Analysis

In this section, the proposed model and the adopted analysis method for the solar energy behavior of the HybE-BS are simulated. Furthermore, the proposed algorithm is simulated and is compared with two previous algorithms described in [22, 23]. The simulation was carried out on the computer with the Intel Pentium dual CPU (3.20GHz), and the proposed algorithm is simulated in MATLAB environment.

In the experiment, the HybE-Net includes 9 HybE-BSs. They are uniformly deployed and are numbered consecutively from left to right and top to bottom, and users are randomly and uniformly distributed. Based on the large experimental results, satisfaction regulatory factor $a = 1000$, parameters of membership functions $\tilde{\sigma}_{j,1} = \tilde{\sigma}_{j,2} = \tilde{\sigma}_{j,3}$=0.14, $b_{j,1} = 0$, $b_{j,2} = 0.5$, $b_{j,3} = 1$; $\tilde{\sigma}_{4,1} = \tilde{\sigma}_{4,5} = 0.18$, $\tilde{\sigma}_{4,2} = \tilde{\sigma}_{4,3}$=$\tilde{\sigma}_{4,4} = 0.2$, $b_{4,1} = -1$, $b_{4,2} = -0.5$, $b_{4,3} = 0$, $b_{4,4} = 0.5$, $b_{4,5} = 1$. To facilitate the analysis, it is assumed that each HybE-BS has the same area of PV panels (3m^2), the same capacity of the battery bank (200Wh) and the same initial energy state (20Wh). Other simulation parameters are given in **Table.2.**

Table 2. System parameters

Parameter	**Value**
Carrier frequency/Bandwidth	2.0GHz/10MHz
Static power consumption P^{sta}	40W
Transmitted power P^{tr}	27dBm
PA efficiency	2/3
Path loss model	Table 6 in [24]
Power spectral density of Gaussian noise σ_0	-174dBm/Hz
Parameters $\mathbb{E}\left[t_m\right]$, $\mathbb{D}\left[t_m\right]$	108，96.7

5.1 Simulation Results of Solar Energy State of HybE-BS

To verify the accuracy of the proposed model and the adopted approximation diffusion analysis, the solar energy state of the HybE-BS is firstly validated. In each group of experiment, different random seeds are adopted to implement experiments for 5000 times, and times for the HybE-BS to reach each energy state at $t = T$ are calculated. Through dividing the statistical number of each energy state with the total times of the experiment, the accumulated probability density of solar energy state of the HybE-BS can be obtained. By taking the average from the 20 groups of experiment results, the accumulated probability density of solar energy state under different access rates λ_m can be obtained as shown in **Fig. 5**. Obviously, the accumulated integral of solar energy states gradually moves right with the increase of access rate λ_m. It is because that the rise of access rate increases the energy consumption rate of the HybE-BS. This phenomenon illustrates that the mean value of solar energy states decreases with the increase of access rate λ_m, which is consistent with the theoretical analysis results. In the meantime, it can be noticed that the accumulated probability density curve obtained from the experiment basically coincides with that from theoretical analysis, proving the accuracy of solar energy states analysis based on the M/G/1/K energy queuing model.

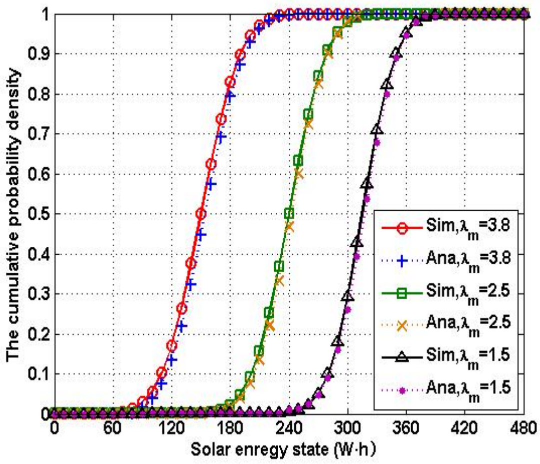

Fig. 5. Cumulative density curve of the solar energy state of the HybE-BS for different access rates

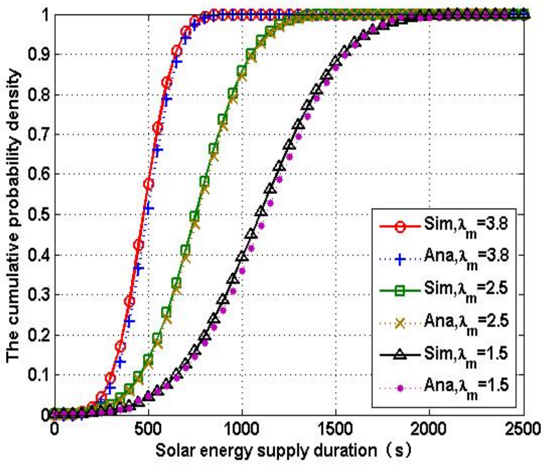

Fig. 6. Cumulative density curve of the duration of solar energy supply for different access rates

Then, the solar energy supply duration is validated by the experiment. Similarly, different random seeds are employed to implement experiments for 5000 times, and the times for the energy state of the HybE-BS to reach $X(t)=0$ during $[0,t]$ are calculated. Through dividing this statistical number with the total times of the experiment, the accumulated probability density of solar energy supply duration of the HybE-BS can be obtained. By taking the average from the 20 groups of experiment results, the accumulated probability density of solar energy supply duration under different access rates λ_m can be obtained as shown in **Fig. 6**. Obviously, the accumulated integral of solar energy supply duration gradually moves left with the increase of access rate λ_m. This phenomenon illustrates that the mean value of solar energy supply duration decreases with the increase of access rate λ_m, which is consistent with the theoretical analysis results. Meanwhile, the accumulated probability density curve obtained from the experiment basically coincides with that from theoretical analysis, proving the accuracy of the adopted analysis method.

At last, the solar energy depleting probability is validated by the experiment. In each group of experiment, different random seeds are adopted to implement experiments for 5000 times, the number of runs that the energy state of the HybE-BS reaches $X(t)=0$ from $X(0)=x_0$ is collected. Through dividing this statistical number with the total times of the experiment, the solar energy depleting probability of the HybE-BS can be obtained. By taking the average from the 20 groups of experiment results, the solar energy depleting probability under different access rates λ_m can be obtained as shown in **Fig. 7.** Obviously, the solar energy depleting probability increases with the increasing of access rate λ_m, and decreases with the increasing of energy harvesting rate λ_e, which is consistent with the theoretical analysis results. Additionally, the analytical results are slightly lower than the simulation results because the observation length is assumed infinity for analysis, while it equals to adjustment period in the simulation.

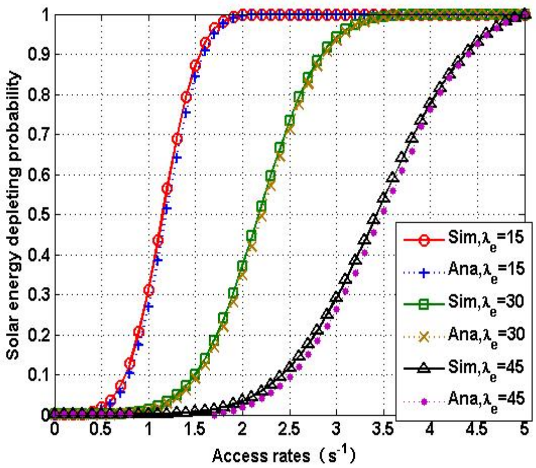

Fig. 7. Solar energy depleting probability of the SEn-BS at different access rates

5.2 Simulation Results of Fuzzy Logic Based Admission Control Algorithm

In order to verify the feasibility and effectiveness of the proposed fuzzy logic based admission control algorithm (FL-ACA), two previous algorithms, the load balance based admission control algorithm (LB-ACA) and the QoS-Aware based admission control algorithm (QA-ACA) are compared in two different simulation scenarios. In “Scenario I”, it is assumed that each HybE-BS has the same energy harvesting rate $\lambda_e = 35\text{J/s}$. However, in “Scenario II”, each HybE-BS has different energy harvesting rates as shown in **Table 3.**

Table 3. Energy harvesting rates of each HybE-BS in “Scenario II”

HybE-BS index	1	2	3	4	5	6	7	8	9
Energy harvesting rate[J/s]	42.2	36.9	41.3	28.4	31.7	32.3	51.4	47.2	34.9

Firstly, we evaluate the performance of the throughput, the index of load balancing and the solar energy utilization balancing for the QA-ACA, LB-ACA, and FL-ACA under two different scenes, as shown in **Fig. 8 (a), (b)** and **(c)**. Specifically, **Fig. 8 (a)** gives the comparisons of the throughput of the three admission control algorithms. It is obvious that the throughput increases with the continuous rise of the number of users. When the number of the user in HybE-Net is small, the throughputs of the QA-ACA, LB-ACA and FL-ACA under two different scenes are all high with tiny differences. However, when the number of the user is large, the throughput of FL-ACA is higher than that of LB-ACA but lower than that of QA-ACA. It is because that QA-ACA stresses the influences of user satisfaction about communication service quality on admission control while FL-ACA and LB-ACA need to consider the traffic load of different HybE-BS, which balances the traffic load of different HybE-BSs in HybE-Net under the premise of satisfying the basic need of communication service quality for user to maximize the system resource utilization. Meanwhile, in FL-ACA, since communication satisfaction is adopted as the input linguistic variables, FL-ACA can guarantee high throughput of HybE-Net under two different defined scenes.

The performance of the index of load balancing at different admission control algorithms is evaluated. Prior to this, the index of load balancing is defined. Similar to the index of solar energy utilization balancing, the index of traffic load balancing θ^w, which is used to measure the load balancing degree of different HybE-BSs, is expresses as:

$$\theta^w = \left(\sum_{i=1}^{I} \xi_i^w\right)^2 \Bigg/ \left(I \cdot \sum_{i=1}^{I} \left(\xi_i^w\right)^2\right), \tag{35}$$

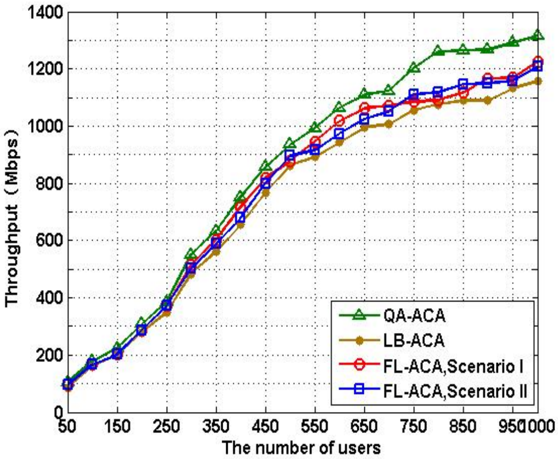

(a)

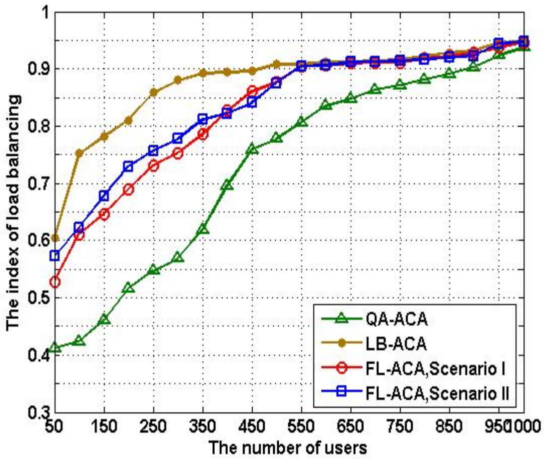

(b)

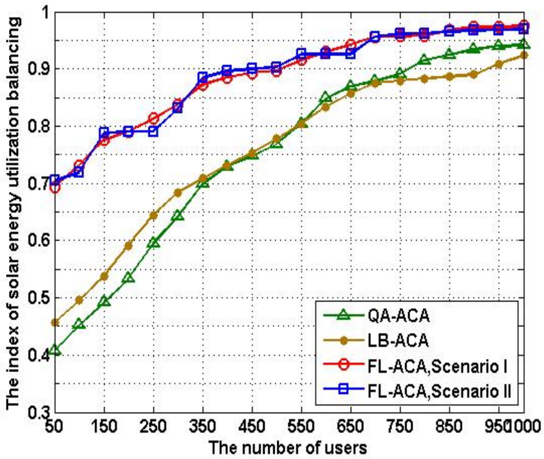

(c)

Fig. 8. Performance evaluation on the throughput, index of load balancing and solar energy utilization balancing for different admission control algorithms. (a) Throughput; (b) The index of load balancing; (c) The index of solar energy utilization balancing

where ξ_i^w represents the available bandwidth ratio of HybE-BS i. It can be concluded that when the traffic load of various HybE-BSs tends to be balanced, θ^w will approach to 1; while when there are huge traffic load differences among various HybE-BSs, θ^w will approach to $1/I$.

As shown in **Fig. 8 (b)**, when the number of user is small, LB-ACA can better improve the index of load balancing; when the number of users reaches a certain number, the differences in the indexes of load balancing of various algorithms are small. This is because that LB-ACA can dynamically predict the traffic load changes and control the access process through analyzing the influence of user accessing different BSs on traffic load balance of the whole network. However, when the number of the user increases, the index of load balancing of various algorithms tends to be stable. The QA-ACA presents the lower index value of the load balancing than other algorithms, without fully considering the load balance problem in user access process. Besides, when the number of users is small, the index of load balancing of the FL-ACA under two different scenes is lower than that of QA-ACA, which is because FL-ACA needs to consider not only the traffic load states of various HybE-BSs but also the solar energy state of various HybE-BSs, in which available bandwidth ratio and the normalized solar energy state of HybE-BS are adopted as the input linguistic variables of the fuzzy logic. However, with the increase of the number of users, the index of load balancing of the FL-ACA under two different scenes approach to that of QA-ACA.

Fig. 8 (c) shows the index of solar energy utilization balancing for QA-ACA, LB-ACA and FL-ACA under two different scenes. It can be observed that FL-ACA is significantly more excellent than QA-ACA and LB-ACA in aspects of solar energy utilization ratio of various HybE-BSs. It is because that FL-ACA analyzes the influences of users accessing different HybE-BSs on the index of solar energy utilization balancing and realizes the balance of solar energy utilization among HybE-BSs. Moreover, it can also be found that even under different energy harvesting rates of different HybE-BSs, FL-ACA algorithm achieve solar energy balance in HybE-Net and effectively improve the solar energy utilization.

Then, the performance of solar energy utilization at different admission control algorithms is evaluated. The solar energy utilization is defined as the proportion of solar energy consumed by HybE-BSs to the total solar energy harvested. It is expressed as:

$$\eta_{\mathrm{E}} = \frac{\sum_{i \in I} E_i^{\mathrm{con}}}{\sum_{i \in I} E_i^{\mathrm{har}}}, \tag{36}$$

where E_i^{con} and E_i^{har} are respectively the solar energy consumed and harvested by HybE-BS i.

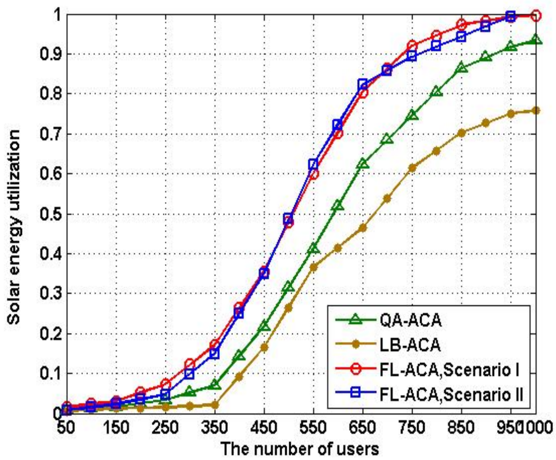

Fig. 9. Comparison of solar energy utilization under different admission control algorithms

Fig. 9 shows the solar energy utilization of QA-ACA, LB-ACA and FL-ACA under two different scenes. Obviously, when the number of users is small, all HybE-BSs in HybE-Net are powered by the solar energy, and there are small differences of solar energy utilization among various algorithms. However, when the number of users is large, the solar energy utilization of QA-ACA and LB-ACA is lower. Consequently, some HybE-BSs are powered by solar energy and others are powered by on-grid energy. This is because that comparison algorithms don’t consider the solar energy state of different HybE-BSs in HybE-Net and cannot control the admission process according to different energy states among different HybE-BSs, which leads to the waste of solar energy resources. In addition, it can also be noticed from **Fig. 9** that FL-ACA has the high solar energy utilization of HybE-Net under two different scenes. It is because that solar energy state of HybE-BS is analyzed in the fuzzy logic, and then users are encouraged to access to the HybE-BS with sufficient solar energy.

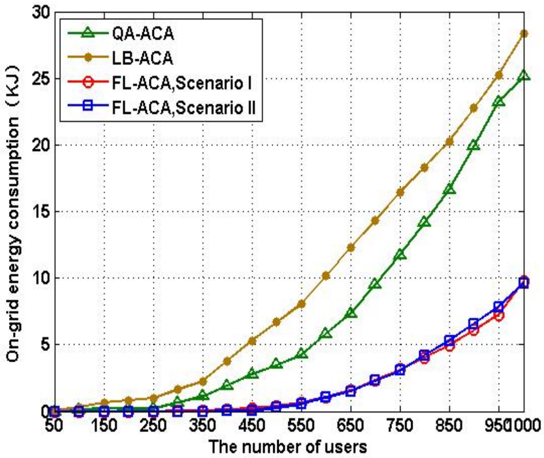

Fig. 10. Comparison of on-grid energy consumption under different admission control algorithms

Finally, **Fig. 10** shows the on-grid energy consumption of QA-ACA, LB-ACA and FL-ACA under two different scenes. It can be easily found that the on-grid energy consumption of the HybE-Net increases with the continuous rise of the number of users. Generally, on-grid energy consumption of FL-ACA is lower than that of QA-ACA and LB-ACA. Particularly, when the number of the user is large, on-grid energy consumption of FL-ACA is far lower than that of other algorithms. Even when solar energy harvesting rates of the HybE-BS are different, FL-ACA can still effectively control user admission according to solar energy utilization and energy state of different HybE-BSs to maximize the solar energy utilization and minimize the on-grid energy consumption. Compared with QA-ACA algorithm, FL-ACA algorithm saves on-grid energy consumption of 5.35KJ, 10.24KJ and 14.27KJ respectively when the number of users is 450, 650 and 850. Compared with LB-ACA algorithm, FL-ACA algorithm saves on-grid energy consumption of 2.65KJ, 6.16KJ and 11.83KJ respectively when the number of users is 450, 650 and 850.

6. Conclusion

In this paper, the cellular network powered by solar energy and on-grid energy is studied, and we proposed a fuzzy logic based admission control algorithm. Firstly, we applied approximation diffusion theory to analyze the solar energy state and dynamic characteristics of the HybE-BS (solar energy duration and solar energy consumption probability). Subsequently, fuzzy logic is utilized to comprehensively consider the access judgment parameters like data transmission rate, system available bandwidth and solar energy state of HybE-BSs. In the meantime, the index of solar energy utilization balancing is proposed to balance the solar energy utilization among different BSs in the proposed algorithm. Finally, the effectiveness of admission control algorithm is proved and the accuracy of modeling and the analysis method on energy behavior in the HybE-BS are verified by the simulation. Simulation results confirmed that the proposed algorithm has a better performance on balancing the load traffic, improving the solar energy utilization among different HybE-BSs and saving on-grid energy. Furthermore, the proposed modeling, analyze method and admission control algorithm also provide a theoretical basis for resource management of other renewable energies powered cellular networks.

Reference

[1] Wang H, Li H, Tang C and et al, "Modeling, metrics, and optimal design for solar energy-powered base station system," *EURASIP Journal on Wireless Communications and Networking*, no. 1, pp. 1-17, January, 2015. Article (CrossRef Link)

[2] Niu Z, Wu Y, Gong J and et al, "Cell zooming for cost-efficient green cellular networks," *IEEE Communications Magazine*, vol. 48, no 11, pp. 74-79, November, 2010. Article (CrossRef Link)

[3] Bhaumik S, Narlikar G, Chattopadhyay S and et al, "Breathe to stay cool: adjusting cell sizes to reduce energy consumption," in *Proc. of 1th ACM Special Interest Group on Data Communication Workshop*, pp. 41-46, August 30-September 3, 2010. Article (CrossRef Link)

[4] 3GPP, "Technical specification group services and system aspects; Telecommunication management; study on energy savings management (Release 9)," *TR 32.826 V1.0.0*, December, 2009. Article (CrossRef Link)

[5] Mancuso V and Alouf S, "Reducing costs and pollution in cellular networks," *IEEE Communications Magazine*, vol. 49, no 8, pp. 63-71, August, 2011. Article (CrossRef Link)

[6] Han T and Ansari N, "On optimizing green energy utilization for cellular networks with hybrid energy supplies," *IEEE Transactions on Wireless Communications*, vol. 12, no 8, pp. 3872-3882, August, 2013. Article (CrossRef Link)

[7] Vergados D D, "Simulation and modeling bandwidth control in wireless healthcare information system," *Simulation Transactions of the Society for Modeling and Simulation International*, vol. 83, no 4, pp. 347-364, April, 2007. Article (CrossRef Link)

[8] Chowdhury M Z, Jang Y M and Haas Z J, "Call admission control based on adaptive bandwidth allocation for wireless networks," *Journal of Communications and Networks*, vol. 15, no 1, pp. 15-24, March, 2013. Article (CrossRef Link)

[9] Cruz-Pérez F, and Ortigoza-Guerrero L, "Flexible resource allocation strategies for class-based QoS provisioning in mobile networks," *IEEE Transactions on Vehicular Technology*, vol. 53, no 3, pp. 805-819, May, 2004. Article (CrossRef Link)

[10] Khanjari S A, Arafeh B, Day K and et al, "An adaptive bandwidth borrowing-based call admission control scheme for multi-class service wireless cellular networks," in *Proc. of Innovations in Information Technology*, pp. 375-380, April 25-27, 2011. Article (CrossRef Link)

[11] Radziemska E, "The effect of temperature on the power drop in crystalline silicon solar cells," *Renewable Energy*, vol. 28, no 1, pp. 1-12, January, 2003. Article (CrossRef Link)

[12] Ng D W K, Lo E S and Schober R, "Energy-efficient resource allocation in OFDMA systems with hybrid energy harvesting base station," *IEEE Transactions on Wireless Communications*, vol. 12, no 7, pp. 3412-3427, July, 2013. Article (CrossRef Link)

[13] Duda A, "Transient diffusion approximation for some queering systems," in *Proc. of Measurement and Modeling of Computer Systems*, pp. 118-128, August, 1983. Article (CrossRef Link)

[14] H. Kobayashi, "Application of the diffusion approximation to queueing networks I: Equilibrium queue distributions," *Journal of the ACM*, vol. 21, no 2, pp. 316-328, April, 1974. Article (CrossRef Link)

[15] Velasquez M and Hester P T, "An analysis of multi-criteria decision making methods," *International Journal of Operations Research*, vol. 10, no 2, pp. 56-66, May, 2013. Article (CrossRef Link)

[16] Xu J and Wu Z, “A discrete consensus support model for multiple attribute group decision making,” *Knowledge-Based Systems*, vol. 24, no 8, pp. 1196-1202, December, 2011. Article (CrossRef Link)
[17] Hussein Y S, Ali B M, Rasid M F A and et al, “Handover in LTE networks with proactive multiple preparation approach and adaptive parameters using fuzzy logic control,” *Ksii Transactions on Internet and Information Systems*, vol. 9, no 7, pp. 2389-2413, July, 2015. Article (CrossRef Link)
[18] Chettibi S, Chikhi S, “Dynamic fuzzy logic and reinforcement learning for adaptive energy efficient routing in mobile ad-hoc networks,” *Applied Soft Computing*, vol. 38, pp. 321-328, January, 2016. Article (CrossRef Link)
[19] Cheng J, Peng C C and Lee C Y, “Identification and prediction using neuro-fuzzy networks with symbiotic adaptive particle swarm optimization,” *Informatica*, vol. 35, no 1, pp. 133-140, March, 2011. Article (CrossRef Link)
[20] Taki M, Heshmati M and Omid Y, “Fuzzy-Based optimized QoS-Constrained resource allocation in a heterogeneous wireless network,” *International Journal of Fuzzy Systems*, pp. 1-10, March, 2016. Article (CrossRef Link)
[21] Johnston R, “Fuzzy logic control,” *Microelectronics Journal*, vol. 26, no 5, pp. 481-495, July, 1995. Article (CrossRef Link)
[22] Ma D and Ma M, “Proactive load balancing with admission control for heterogeneous overlay networks,” *Wireless Communications and Mobile Computing*, vol. 13, no 18, pp. 1671-1680, November, 2011. Article (CrossRef Link)
[23] Saidu I, Subramaniam S, Jaafar A and et al, “A QoS-Aware CAC with bandwidth reservation and degradation scheme in IEEE 802.16 e networks,” *Wireless Personal Communications*, vol. 82, no 4, pp. 2673-2693, June, 2015. Article (CrossRef Link)
[24] 3GPP, “RAN4: Simulation assumptions and parameters for FDD HeNB RF requirements,” *R4-092042*, May, 2009. Article (CrossRef Link)

Heng Wang received his M.S. and Ph.D. degrees in communication and information system from Chongqing University in 2012 and 2015, respectively. Now, he is an assistant professor with college of Mechanical and Electrical Engineering of Henan Agricultural University. His current research interests include green communications and cognitive networks.

Chaowei Tang received his B.S., M.S. and Ph.D. degrees in communication and information system from Chongqing University in 1987, 1990 and 1993 separately. Now he is a professor in college of Communication engineering, Chongqing University. His research interests include green communications, computer vision, data mining and Internet of things.

Zhenzhen Zhao received his M.S. and Ph.D. degrees in circuit and system from Chongqing University in 2012 and 2016 separately. Now, she is an assistant professor with college of Computer and Information Engineering of Henan University of Economics and Law. Her research interests cover advanced mobile communication systems and the key technologies, including heterogeneous network, green communications.

Hui Tang received his B.S. degree from Lanzhou University in 1992, his M.S. degree from the Institute of Computing Technology of the Chinese Academy of Sciences in 1995, and his Ph.D. degree from the Institute of Acoustics of the Chinese Academy of Sciences in 1998. Since 2004 he has become the founding director of the High Performance Network Laboratory of the Institute of Acoustics of the Chinese Academy of Sciences. His research interest is the next-generation broadband wireless mobile network.